Acta Crystallographica Section B
**Structural
Science**
ISSN 0108-7681

Structure of $KNbOB_2O_5$ – a commensurately modulated structure

Siegbert Schmid[a]* and Trixie Wagner[b]

[a]School of Chemistry, The University of Sydney, Sydney, NSW 2006, Australia, and [b]Novartis Institutes for Biomedical Research, WSJ-503.12.08, 4002 Basel, Switzerland

Correspondence e-mail:
s.schmid@chem.usyd.edu.au

Received 23 August 2004
Accepted 12 May 2005

Members of the $AMOB_2O_5$ (A = K, Rb, Cs, Tl; M = Nb, Ta) family of compounds can be described as modulated structures with a single superspace group and very similar modulation functions. Single-crystal X-ray diffraction data (Mo $K\alpha$ radiation) are used to solve and refine the structure of $KNbOB_2O_5$ in these terms for the first time. The average structure is solved and refined in the space group $Pmn2_1$. Subsequently, the atomic modulation functions are determined using *JANA*2000 and superspace-group symmetry $Pmn2_1(0,0.375,0)s$. The commensurately modulated structure is finally refined as a superstructure in the space group $Pbn2_1$ using *SHELXS*97 converging to $R_1 = 0.024$.

1. Introduction

Modulated structures have been encountered for many decades (van Smaalen, 1995), but only since the development of superspace group theory (Janner & Janssen, 1977; Perez-Mato *et al.*, 1987) and software that can handle modulated structures efficiently (Petříček *et al.*, 2004) has their study become more of a mainstream effort. Prior to that modulated structures were often approximated by medium or long-period superstructures. While these approximations were often very reasonable, nevertheless, they did not represent the best possible model for the compounds in question (Schmid & Withers, 1996).

One example for such a case is the family of non-centrosymmetric oxo pyroborates, $AMOB_2O_5$ (A = K, Rb, Cs, Tl; M = Nb, Ta; Gasperin, 1974; Baucher & Gasperin, 1975; Baucher *et al.*, 1976; Akella & Keszler, 1995; Becker *et al.*, 1995; Gopalakrishnan *et al.*, 1999; Nicholls *et al.*, 2001). Some of these compounds attracted considerable interest owing to their potential use as non-linear optical materials. All members of the family form structures that are based on a common underlying basic structure. In addition, most exhibit superstructures of varying multiplicities along the b axis, corresponding to the $Pmn2_1$ setting of $CsNbOB_2O_5$ (Becker *et al.*, 1995), which was reported without superstructure, *i.e.* it represents the basic structure type (Akella & Keszler, 1995; Becker *et al.*, 1995). $CsTaOB_2O_5$ has been reported with an eightfold superstructure (Becker *et al.*, 1995) and without (Akella & Keszler, 1995), but it is unclear whether these are in fact two modifications. The Tl compound, $TlNbOB_2O_5$ (Gasperin, 1974), displays a twofold superstructure and the Rb compound, $RbNbOB_2O_5$ (Baucher *et al.*, 1976), a fivefold superstructure.

Recently, a modulated structure approach was used to re-refine the structure of $RbNbOB_2O_5$ (Schmid *et al.*, 2000). Starting values for the displacive modulation wave amplitudes

doi:10.1107/S0108768105016393

used in the refinement were derived from the previously reported superstructure refinement. Refinement in terms of modulation waves proved to be very stable and resulted in an improved crystal chemical description. The overall *R* value for the modulated structure refinement was substantially lower than for the superstructure refinement, whilst employing a significantly reduced number of positional parameters.

The synthesis of $KNbOB_2O_5$ was first reported by Becker in 1991 (Becker *et al.*, 1991), including the observation from Buerger precession photographs that an eightfold superstructure was formed. A few years later that compound was reported again (Nicholls *et al.*, 1993) and over the next five years three more publications from the same group appeared (Nicholls *et al.*, 1997, 2000, 2001). While their interest was mainly on the optical properties and applications in lasers and non-linear optical devices, they reported a structure for $KNbOB_2O_5$. No data were given, however, that would have allowed an independent check of that structure. Furthermore, between the first and last of these publications the space-group assignment changed twice, without any explanation. In all of these publications it was claimed that the space groups for both the Rb and K compounds are the same, however, it will be shown below that this is incorrect. Given the immense interest in the properties of this material coupled with the limited and inconclusive crystallographic information available and the results from the Rb analogue it seemed appropriate and timely to examine the structure of $KNbOB_2O_5$ using a superspace approach.

While a previous superstructure refinement had been performed on $RbNbOB_2O_5$, there were no such data available for $KNbOB_2O_5$. Therefore, it seemed particularly challenging to test the superspace approach for this compound.

2. Experimental

2.1. Data collection and processing

$KNbOB_2O_5$ crystals used for data collection were provided by Dr B. Chai from the Centre for Research and Education in Optics and Lasers at the University of Central Florida (Nicholls *et al.*, 1993). A complete intensity data set was measured on a Bruker SMART APEX CCD diffractometer (Schmid *et al.*, 2002). The crystal used for that data collection was a transparent plate of approximate dimensions 0.23 × 0.23 × 0.18 mm. In addition, data were collected on a Nonius KappaCCD diffractometer to allow the reconstruction of the images of the reciprocal layers, which clearly show the effects of the modulation (see Figs. 1 and 2).

The crystal mounted on a glass fibre was aligned on a Bruker SMART APEX CCD diffractometer. Preliminary lattice parameters and an orientation matrix were obtained from three sets of frames and refined during the integration process of the intensity data. Intensity measurements were performed using graphite-monochromated Mo $K\alpha$ radiation from a sealed tube and a monocapillary at 293 K with the ω scan method (Bruker, 1999*a*). Data were processed using *SAINT* (Bruker, 1999*b*). A semi-empirical absorption correction was applied, based on the intensities of symmetry-related reflections measured at different angular settings (Sheldrick, 1996). During data processing it became evident that the crystal showed exact eightfold multiplicity along *b*, consistent with previous reports (Becker *et al.*, 1995).

2.2. Symmetry considerations

Much of the discussion on symmetry for $KNbOB_2O_5$ is analogous to the equivalent discusion for $RbNbOB_2O_5$ (Schmid *et al.*, 2000). Consequently, the following contains

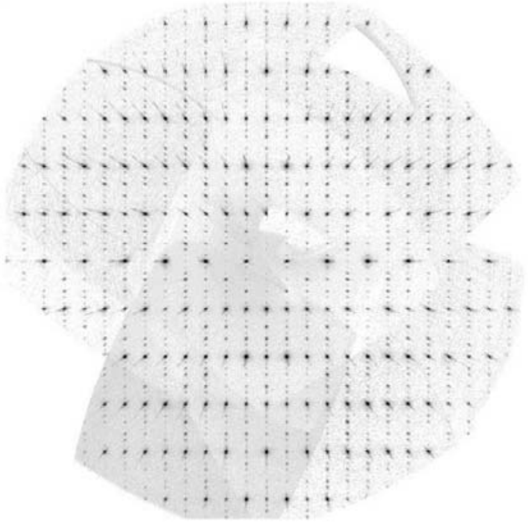

Figure 1
Reconstructed image of the [1*kl*] zone axis of $KNbOB_2O_5$. Between the very strong main reflections, corresponding to the underlying substructure, there are up to seven satellite reflections, resulting in an eightfold superstructure. The third and fifth satellite reflections are systematically much stronger than the others (**b*** up the page).

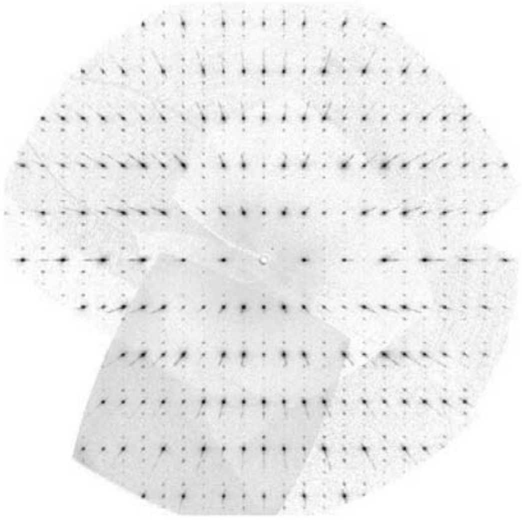

Figure 2
Reconstructed image of the [0*kl*] zone axis of $KNbOB_2O_5$. The very strong main reflections correspond to the underlying substructure. Comparison with Fig. 1 shows that only every second reflection is present along **b***, *i.e.* reflections with 0*kl*, $k \neq 2n$ (or 0*klm*, $m \neq 2n$) are systematically extinct (**b*** up the page).

Table 1
Experimental details.

Crystal data	
Chemical formula	$B_8K_4Nb_4O_{24}$
M_r	3994.08
Cell setting, space group	Orthorhombic, $Pbn2_1$
a, b, c (Å)	7.3056 (11), 31.1632 (18), 9.1659 (15)
V (Å^3)	2086.8 (5)
Z	4
D_x (Mg m^{-3})	3.178
Radiation type	Mo $K\alpha$
No. of reflections for cell parameters	928
θ range (°)	1.31–26.47
μ (mm^{-1})	3.06
Temperature (K)	293 (2)
Crystal form, colour	Block, colourless
Crystal size (mm)	0.23 × 0.23 × 0.18
Data collection	
Diffractometer	Three-circle goniometer
Data collection method	ω scans
Absorption correction	Multi-scan
No. of measured, independent and observed reflections	12 617, 4272, 3768
Criterion for observed reflections	$I > 2\sigma(I)$
R_{int}	0.021
$\theta_{\max}$ (°)	26.5
Range of h, k, l	$-9 \Rightarrow h \Rightarrow 6$ $-39 \Rightarrow k \Rightarrow 36$ $-11 \Rightarrow l \Rightarrow 11$
Refinement	
Refinement on	F^2
$R[F^2 > 2\sigma(F^2)]$, $wR(F^2)$, S	0.024, 0.065, 0.97
No. of reflections	4272
No. of parameters	362
Weighting scheme	$w = 1/[\sigma^2(F_o^2) + (0.0365P)^2]$, where $P = (F_o^2 + 2F_c^2)/3$
$(\Delta/\sigma)_{\max}$	0.189
$\Delta\rho_{\max}$, $\Delta\rho_{\min}$ (e Å^{-3})	0.40, −0.57
Extinction method	*SHELXL*
Extinction coefficient	0.00051 (5)
Absolute structure	Flack (1983)
Flack parameter	0.02 (4)

Computer programs used: *SHELXS*97 (Sheldrick, 1997*a*), *SHELXL*97 (Sheldrick, 1997*b*).

only the arguments that are necessary to appreciate the differences and similarities between these two structures.

Fig. 1 shows a reconstructed image (Nonius KappaCCD data) of the [1*kl*] zone axis of $KNbOB_2O_5$ (**c*** to the right, **b*** up the page). The strong reflections of the underlying average structure are separated by seven satellite or superstructure reflections, giving rise to an exact eightfold multiplicity along **b**. The primary modulation wavevector has been chosen to be $(3/8)\mathbf{b}_p^*$ rather than $(1/8)\mathbf{b}_p^*$, because the $\mathbf{G}_p \pm (3/8)\mathbf{b}_p^*$ satellite reflections are invariably stronger than the other satellite reflections (Perez-Mato *et al.*, 1987). The one exception to this rule is at the [0*kl*] zone axis of Fig. 2, where the even-order harmonic $\mathbf{G}_p \pm (2n/8)\mathbf{b}_p^*$ satellite reflections are still weak, but where the odd-order $\mathbf{G}_p \pm (2n + {}^1/_8)\mathbf{b}_p^*$ satellite reflections are systematically absent.

The same extinction condition [*i.e.* $F(0klm) = 0$ unless m is even] was previously observed for $RbNbOB_2O_5$. For a modulation wavevector of $(2/5)\mathbf{b}_p^*$, as in $RbNbOB_2O_5$, that condition does not lead to a three-dimensional extinction condition, whereas for a modulation wavevector of $(3/8)\mathbf{b}_p^*$, as in the present case, it is consistent with a b-glide extinction condition. A further feature is the characteristic extinction condition [$F(h0l0) = 0$ unless $h + l$ is even] which is apparent in Figs. 1 and 2. Such an extinction condition implies the existence of a superspace-symmetry operator of the form $\{x_1 + \frac{1}{2}, -x_2, x_3 + \frac{1}{2}, -x_4 + 2\delta\}$. Taken together with the $\{-x_1, x_2, x_3, x_4 + \frac{1}{2}\}$ symmetry operator required by the first extinction condition, the overall implied superspace group symmetry is thus $Pmn2_1(0,0.375,0)s$.

For a commensurate modulated structure with $\mathbf{q} = (3/8)\mathbf{b}^*$ (as in the current case), the choice of global phase parameter δ in conjunction with the superspace-group symmetry determines the resultant conventional three-dimensional space-group symmetry (Yamamoto & Nakazawa, 1982; Wiegers *et al.*, 1990; Perez-Mato, 1991; van Smaalen, 1995). The possible three-dimensional supercell space-group symmetries for $KNbOB_2O_5$ are given by $Pbn2_1$ [for $\delta = (2n/16)$, n an integer], $Pbn2_1$ with a different origin choice [for $\delta = (2n + 1)/16$] and $Pb11$ (otherwise). These possible space groups are different to those for $RbNbOB_2O_5$ (Schmid *et al.*, 2000) and are not consistent with the results of Nicholls *et al.* (1993, 1997, 2000, 2001).

If there is no 'overlap', these various possibilities cannot be distinguished from the refinement point of view (Perez-Mato, 1991) and will give identical reciprocal space intensity distributions and hence identical Patterson maps despite being structurally distinct in the conventional three-dimensional crystallographic sense. Such structures were labelled homometric (Patterson, 1939). The definition of 'no overlap' is that significantly less than the maximum number of higher-order harmonic satellite reflections possible are ever observed, so it is always clear to which average structure Bragg reflection **G** a particular satellite reflection belongs.

2.3. Refinement details

An initial structure solution with direct methods was carried out using *SHELXS*97 (Sheldrick, 1997*a*). While this approach yielded the average structure using only the main reflections (in the space group $Pmn2_1$), it failed for the superstructure, owing to the large number of either weak or unobserved satellite reflections. That average structure solution was then taken as the starting model for the modulated structure refinement using *JANA*2000 (Petříček *et al.*, 2004). First- to fourth-order coefficients of the displacive modulation waves were added consecutively and the signs checked by systematically reversing them in comparative refinements. As at least fourth-order satellites were observed, whether there was 'overlap' between satellite reflections or not needed to be investigated. While the initial refinements were carried out in an incommensurate setting the final cycles were run as a commensurately modulated structure with a range of δ values. The commensurate formalism significantly improved the final refinements for all values of δ and this demonstrates that there

Table 2
Selected bond lengths (Å) for $KNbOB_2O_5$.

K1—O(2–5)^{i}	2.756 (3)	K2—O(2–2)^{ii}	2.817 (3)	K3—O(1–2)^{iii}	2.853 (3)
K1—O(3–4)^{iii}	2.825 (3)	K2—O(3–3)^{iii}	2.848 (3)	K3—O(1–6)	2.859 (3)
K1—O(1–4)^{iii}	2.853 (3)	K2—O(1–7)^{iv}	2.859 (3)	K3—O(3–2)^{iii}	2.904 (3)
K1—O(1--8)^{iv}	2.859 (3)	K2—O(1–3)^{iii}	2.920 (3)	K3—O(2–7)^{i}	2.957 (3)
K1—O(1–7)^{iv}	2.999 (3)	K2—O(3–2)^{iii}	3.018 (3)	K3—O(2–3)^{iv}	3.029 (3)
K1—O(3–3)^{iii}	3.043 (3)	K2—O(2–3)^{iii}	3.096 (3)	K3—O(2–6)^{iv}	3.106 (3)
K1—O(4–4)^{iii}	3.262 (2)	K2—O(1–2)^{iii}	3.101 (3)	K3—O(3–1)^{iii}	3.111 (3)
K1—O(2–8)^{iv}	3.342 (3)	K2—O(2–6)^{i}	3.288 (3)	K3—O(1–1)^{iii}	3.176 (3)
K1—O(2–1)^{ii}	3.404 (3)	K2—O(4–3)^{v}	3.385 (3)	K3—O(2–2)^{ii}	3.313 (3)
K4—O(1–5)^{iv}	2.774 (3)				
K4—O(1–1)^{iii}	2.803 (3)				
K4—O(2–8)^{i}	2.871 (3)				
K4—O(3–1)^{iii}	2.919 (3)				
K4—O(1–4)^{iv}	3.034 (3)				
K4—O(3–4)^{iv}	3.117 (3)				
K4—O(2–4)^{iv}	3.143 (3)				
K4—O(2–7)^{i}	3.249 (3)				
K4—O(2–1)^{iii}	3.275 (3)				
K4—O(4–1)^{iii}	3.418 (3)				
Nb1—O(4–1)	1.769 (2)	Nb2—O(4–2)	1.755 (2)	Nb3—O(4–3)	1.770 (2)
Nb1—O(2–1)	1.924 (3)	Nb2—O(2–2)	1.946 (3)	Nb3—O(2–7)^{vi}	1.949 (3)
Nb1—O(2–5)^{vi}	1.944 (3)	Nb2—O(2–6)^{vi}	1.951 (3)	Nb3—O(2–3)	1.963 (3)
Nb1—O(1–5)^{vi}	1.967 (3)	Nb2—O(1–2)	1.991 (3)	Nb3—O(1–3)	1.984 (3)
Nb1—O(1–1)	2.031 (3)	Nb2—O(1–6)^{vi}	2.010 (3)	Nb3—O(1–7)^{vi}	2.023 (3)
Nb1—O(4–2)	2.201 (2)	Nb2—O(4–3)	2.208 (2)	Nb3—O(4–4)	2.2223 (1)
Nb4—O(4–4)	1.7740 (19)				
Nb4—O(2–4)	1.938 (3)				
Nb4—O(2–8)^{vi}	1.955 (3)				
Nb4—O(1–8)^{vi}	1.962 (3)				
Nb4—O(1–4)	2.041 (3)				
Nb4—O(4–1)^{vii}	2.212 (2)				
B1—O(2–1)	1.329 (5)	B2—O(1–2)^{viii}	1.344 (5)	B3—O(1–1)^{viii}	1.340 (5)
B1—O(1–3)^{viii}	1.345 (5)	B2—O(2–2)	1.355 (5)	B3—O(2–3)	1.359 (5)
B1—O(3–1)	1.396 (4)	B2—O(3–2)	1.384 (5)	B3—O(3–3)	1.407 (4)
B4—O(2–4)	1.335 (5)	B5—O(2–5)	1.354 (5)	B6—O(2–6)	1.339 (5)
B4—O(1–8)^{ix}	1.346 (5)	B5—O(1–7)^{ix}	1.354 (5)	B6—O(1–6)^{ix}	1.350 (5)
B4—O(3–4)	1.392 (4)	B5—O(3–1)^{x}	1.383 (5)	B6—O(3–2)^{x}	1.404 (5)
B7—O(1–5)^{ix}	1.345 (5)	B8—O(1–4^{ix}	1.339 (5)		
B7—O(2–7)	1.345 (5)	B8—O(2–8)	1.353 (5)		
B7—O(3–3)^{x}	1.398 (5)	B8—O(3–4)^{x}	1.395 (5)		

Symmetry codes: (i) $1-x, y-\frac{1}{2}, z-1$; (ii) $x, y, z-1$; (iii) $2-x+\frac{1}{2}, -y+\frac{1}{2}, z-\frac{1}{2}$; (iv) $x-\frac{1}{2}, -y+1, z-\frac{1}{2}$; (v) $-x-\frac{1}{2}, -y+\frac{1}{2}, z-\frac{1}{2}$; (vi) $-x, y-\frac{1}{2}, z$; (vii) $-x, y+\frac{1}{2}, z$; (viii) $-x+\frac{1}{2}, -y+\frac{1}{2}, z+\frac{1}{2}$; (ix) $-x+\frac{1}{2}, -y+\frac{3}{2}, z+\frac{1}{2}$; (x) $-x+1, y+\frac{1}{2}, z$.

is indeed 'overlap'. For δ values of 0 and multiples of (1/16), the space group $Pbn2_1$ results in different origin choices, otherwise the space group $Pb11$ is realized (see above). The former case proved to be the best option. Subsequently, the positional parameters were calculated for all atoms in the corresponding superstructure (with $\delta = 0$). While *JANA*2000 is the program of choice for all modulated structure refinements, there is a range of suitable programs to carry out a final superstructure refinement (including *JANA*2000). In the present case the final refinement was carried out using *SHELXL*97 (Sheldrick, 1997*b*) and the resulting model is discussed below. Table 1 gives the crystal data and refinement parameters for the final refined structure, while Table 2 gives selected bond lengths. Atomic coordinates and equivalent isotropic displacement parameters have been deposited.[1]

3. Results and discussion

The solution and refinement of the $KNbOB_2O_5$ structure reported here has demonstrated one significant advantage of the modulation-wave approach. It allows a hierarchical approach to structure refinement, starting with the refinement of the average structure using only the parent reflections followed by refinement of the first harmonic displacive modulation wave amplitudes using parent and first-order satellite reflections *etc.* (Schmid & Withers, 1995, 1996). Such an approach avoids many of the instabilities associated with conventional long period superstructure refinements where no such hierarchy exists. Provided fractional coordinates in the large supercell are then calculated from the results of the commensurate modulated structure refinement a final superstructure refinement can still be used and will usually give rather similar refinement statistics (Perez-Mato, 1991). Allowing only the appropriate limited number of higher-order harmonics in the modulated structure refinement will usually avoid high frequency noise, which is an unavoidable consequence of conventional long-period superstructure refinements. From the three-dimensional space groups given in the preceding paragraph it is also clear that symmetry lowering from orthorhombic to monoclinic can occur for some choices of the global phase. The intensity distribution in reciprocal space does not support such lowering of symmetry and a conventional refinement must therefore suffer from severe correlation problems as well as the neglect of some of the structural features. It is worth noting that the space group reported by Nicholls *et al.* (2001) indeed had monoclinic symmetry. Refinement as a commensurately modulated structure will preserve the higher symmetry and even if that is slightly broken, it will still give the better model since it avoids the high-frequency noise usually present in such long-period superstructure refinements. It needs to be considered, however, that the superspace-group symmetry is only an approximation (Janssen *et al.*, 1992), albeit a very good one.

By employing the modulation wave approach it has been possible to arrive at a final superstructure model that refines extremely well and does not show any unusual features. The projection of the average structures in Fig. 3 shows that there

---

[1] Supplementary data for this paper are available from the IUCr electronic archives (Reference: CK5006). Services for accessing these data are described at the back of the journal.

are clearly very anisotropic atomic displacement parameters, owing to the modulation of the real structure. That structure is shown in projection down **b** in Fig. 4 and down **c** in Fig. 5. The similarity with the structure of the Rb compound is striking, particularly in projection down *b*. In that figure the niobium oxygen octahedra are also slightly rotated around the *b* axis, while in Fig. 5 the same tilting is visible that was observed in the Rb analogue. It is readily seen that the apical O atoms of the niobium oxygen octahedra are strongly displaced from the average position along **a**, leading to a meander arrangement of the chain along **b**. The boron ions are mainly displaced along the *b* direction, which is in stark contrast to Nicholls *et al.* (2001), who describe an almost planar network of $(B_2O_5)^{4-}$ groups. This projection also shows the large channels, which are formed by the niobium oxygen octahedra connected *via* pyroborate groups, and accommodate the large *A* cations. The niobium oxygen octahedra show no unusual features. Niobium sits above the basal plane resulting in one shorter (~ 1.767 Å) and one longer bond (~ 2.211 Å) along the chain direction. This is the result of a second-order Jahn–Teller effect, characteristic for d^0 transition metals, which mixes the cationic LUMO and anionic HOMO states, stabilizing a distorted NbO_6 octahedron (Wheeler *et al.*, 1986; Kunz & Brown, 1995). The other four bonds in the basal plane of each octahedron are intermediate, ranging from 1.924 to 2.041 Å. All the Nb—O distances are in very good agreement with those found for the unmodulated $CsNbOB_2O_5$ structure (Becker *et al.*, 1995). Boron is coordinated by three O atoms with two shorter bonds (~ 1.346 Å) to the O atoms in the octahedra and one longer bond (~ 1.395 Å) to the oxygen that is only bonded to two B atoms. Again, these distances are in good agreement with the $CsNbOB_2O_5$ structure (Becker *et al.*, 1995). The coordination around potassium is, as in the rubidium case, quite irregular, showing the largest deviation from the distances in the caesium compound and compared with the average structure. Starting with the shortest distances to oxygen of ~ 2.76 Å, the coordination numbers range from 7 to 9 if a cut-off of 3.3 Å is chosen, with 34 bond lengths across this range (Table 2). This almost resembles a continuum as seen in incommensurately modulated structures (*e.g.* $RbNbOB_2O_5$; Schmid *et al.*, 2000). There is no apparent large gap in these bond distances that would justify defining a first coordination sphere. The observed flexibility in the potassium coordination polyhedra is consistent with other reported structures, *e.g.* two potassium

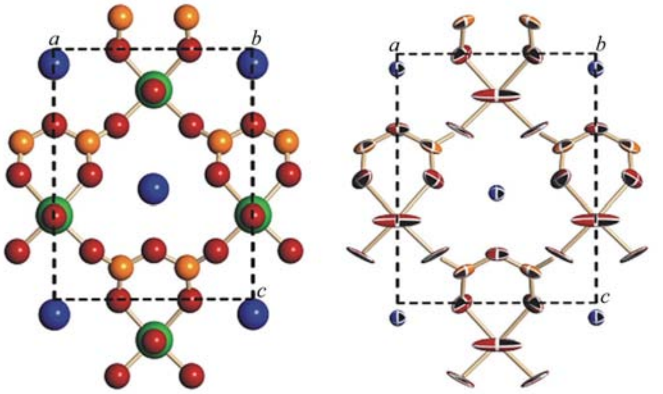

Figure 3
Projection of the basic structure of $KNbOB_2O_5$ along *b*. Despite a low *R* value ($R_1 = 0.028$) for the basic structure (in the space group $Pmn2_1$), the displacement ellipsoids in the right part of the picture clearly show that there are inherent problems owing to the modulation (see below).

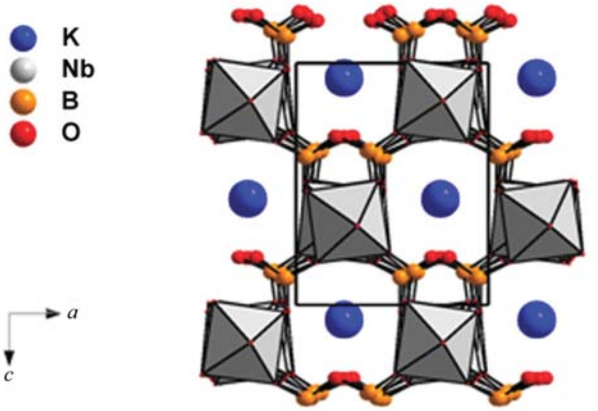

Figure 4
Projection of the real structure of $KNbOB_2O_5$ along *b*. The unit cell is outlined (space group $Pbn2_1$). It can be clearly seen that the octahedra are rotated against each other with respect to the *b* axis. Compare the displacive modulation of the O atoms in the B_2O_5 groups to the atomic displacement parameters in the right-hand part of Fig. 3.

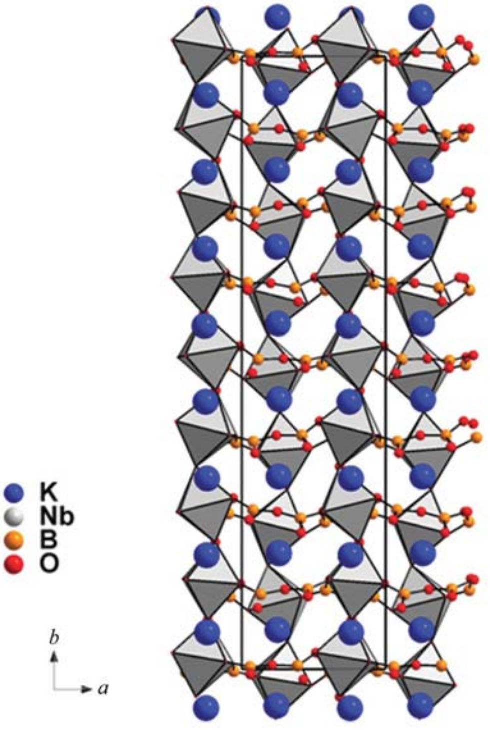

Figure 5
Projection of the real structure of $KNbOB_2O_5$ along *c*. The unit-cell edges are shown. It can be clearly seen that the niobium oxygen octahedra are tilted strongly along *a*, resulting in a meander arrangement of the chains along *b*.

borates with coordination numbers from 7 to 10 and K—O distances from 2.691 to 3.267 Å, which were reported recently (Zhang *et al.*, 2005).

Apparent valence calculations (Brown & Altermatt, 1985) are a powerful tool to examine the plausibility of refined crystal structures and are particularly helpful when irregular coordination polyhedra (see above) are formed in the structure. In order to shed some light on the formation of modulated structures in the $AMOB_2O_5$ family of compounds, bond-valence sums were calculated for $KNbOB_2O_5$. As in the case of $RbNbOB_2O_5$ (Schmid *et al.*, 2000), where all apparent valence sums were close to the expected values, the calculated values (averages given) are within error of the expected value for all the metal atoms in the structure (K: 0.9; Nb: 5.3; B: 3.1). In the average structure the apparent valences for Nb and B are higher (5.7 and 3.3), while the apparent valence for K is slightly lower (0.8). For comparison purposes bond-valence sums were also calculated for the unmodulated Cs member of this family, as well as hypothetical structures where Cs was substituted by K, Rb or Tl. The resulting values were Cs (1.0), Tl (0.5), Rb (0.6) and K (0.4). These numbers may hold the key to understanding the modulation. Caesium, the largest *A* cation in this family, is adequately bonded and forms an unmodulated structure. The undistorted channels formed by the framework, however, are too large to provide the remaining *A* ions with an adequate bonding environment. Instead the modulation in those compounds reduces the size of the channels to fit rubidium, thallium and potassium. If they were to form the same structure as Cs, with untilted niobium oxygen octahedra, all of them would be significantly underbonded.

4. Conclusion

The structure of $KNbOB_2O_5$, which adapts an eightfold superstructure, was successfully solved and refined using a mixed conventional/superspace approach. Using average structure positions and refined atomic modulation functions it was possible to calculate and refine accurate atomic positional parameters in a superstructure model. This approach avoids problems in the refinement caused by often large numbers of either weak or unobserved satellite reflections and might be used more generally. For the refined structures of both $RbNbOB_2O_5$ (Schmid *et al.*, 2000) and $KNbOB_2O_5$ the apparent valence calculations show that rubidium and potassium, respectively, are satisfactorily bonded, providing a key to understanding the cause of the modulation. Caesium, the largest *A* ion in this family, forms an unmodulated structure. The undistorted channels formed by the framework, however, are too large to provide the smaller ions with an adequate bonding environment. Instead the modulation reduces the size of the channels to fit those ions.

The authors thank Dr M. Adam, Bruker AXS for providing the diagrams used in Figs. 1 and 2.

References

Akella, A. & Keszler, D. A. (1995). *J. Solid State Chem.* **120**, 74–79.

Baucher, A. & Gasperin, M. (1975). *Mater. Res. Bull.* **10**, 469–472.

Baucher, A., Gasperin, M. & Cervelle, B. (1976). *Acta Cryst.* B**32**, 2211–2215.

Becker, P., Bohatý, L. & Fröhlich, R. (1991). *Eur. J. Mineral.* **3**, 22.

Becker, P., Bohatý, L. & Fröhlich, R. (1995). *Acta Cryst.* C**51**, 1721–1723.

Brown, I. D. & Altermatt, D. (1985). *Acta Cryst.* B**41**, 244–247.

Bruker (1999*a*). *SMART*. Bruker AXS Inc., Madison, Wisconsin, USA.

Bruker (1999*b*). *SAINT*. Bruker AXS Inc., Madison, Wisconsin, USA.

Flack, H. D. (1983). *Acta Cryst.* A**39**, 876–881.

Gasperin, M. (1974). *Acta Cryst.* B**30**, 1181–1183.

Gopalakrishnan, J., Ramesha, K. R. K. & Pandey, S. (1999). *J. Solid State Chem.* **148**, 75–80.

Janner, A. & Janssen, T. (1977). *Phys. Rev. B*, **15**, 643–658.

Janssen, T., Janner, A., Looijenga-Vos, A. & de Wolff, P. M. (1992). *International Tables for Crystallography*, edited by A. J. Wilson, pp. 797–835. Kluwer Academic Publishers, Dordrecht, The Netherlands.

Kunz, M. & Brown, I. D. (1995). *J. Solid State Chem.* **115**, 395–406.

Nicholls, J. F. H., Chai, B. H. T., Corker, D. L., Calabrese, J. C. & Henderson, B. (1993). Proc. of SPIE-The International Society for Optical Engineering, Vol. 1863, pp. 54–59. July, Florida.

Nicholls, J. F. H., Henderson, B. & Chai, B. H. T. (1997). *Opt. Mater. (Amsterdam)*, **8**, 215–226.

Nicholls, J. F. H., Henderson, B. & Chai, B. H. T. (2001). *Opt. Mater.* **16**, 453–462.

Nicholls, J. F. H., Henderson, B., Gallagher, H. G. & Chai, B. H. T. (2000). *J. Cryst. Growth*, **220**, 263–274.

Patterson, A. L. (1939). *Nature*, **143**, 939–940.

Perez-Mato, J. M. (1991). *Methods of Structural Analysis of Modulated Structures and Quasicrystals*, edited by J. M. Perez-Mato, F. J. Zuniga & G. Madariaga, pp. 117–218. Singapore: World Scientific.

Perez-Mato, J. M., Madariaga, G., Zuniga, F. J. & Arribas, A. G. (1987). *Acta Cryst.* A**43**, 216–226.

Petříček, V., Dušek, M. & Palatinus, L. (2004). *JANA*2000. Institute of Physics, Praha, Czech Republic.

Schmid, S., Wagner, T. & Adam, M. (2002). *Z. Kristallogr.* Suppl. **19**, 96.

Schmid, S. & Withers, R. L. (1995). *Acta Cryst.* B**51**, 746–753.

Schmid, S. & Withers, R. L. (1996). *Aust. J. Chem.* **49**, 827–833.

Schmid, S., Withers, R. L., Corker, D. & Baules, P. (2000). *Acta Cryst.* B**56**, 558–564.

Sheldrick, G. M. (1996). *SADABS*. University of Göttingen, Germany.

Sheldrick, G. M. (1997*a*). *SHELXS*97. University of Göttingen, Germany.

Sheldrick, G. M. (1997*b*). *SHELXL*97. University of Göttingen, Germany.

Smaalen, S. van (1995). *Cryst. Rev.* **4**, 79–202.

Wheeler, R. A., Whangbo, M.-H., Hughbanks, T., Hoffman, R., Burdett, J. K. & Albright, T. A. (1986). *J. Am. Chem. Soc.* **108**, 2222–2236.

Wiegers, G. A., Meetsma, A., Haange, R. J., van Smaalen, S., de Boer, J. L., Meerschaut, A., Rabu, P. & Rouxel, J. (1990). *Acta Cryst.* B**46**, 324–332.

Yamamoto, A. & Nakazawa, H. (1982). *Acta Cryst.* A**38**, 79–86.

Zhang, H.-X., Zhang, J., Zheng, S.-T. & Yang, G.-Y. (2005). *Cryst Growth Des.* **5**, 157–161.